Hindawi
Journal of Food Biochemistry
Volume 2023, Article ID 2180179, 15 pages
https://doi.org/10.1155/2023/2180179

Research Article

Structural Characterization and Antifatigue Activity of a Novel Exopolysaccharide Isolated from *Marasmius androsaceus*

Peng Du,[1] **Nan Li**,[1,2] **Junqing Wang**,[1] **Piwu Li**,[1] **Jia Song**,[2] **Xiaoqi Geng**,[3] **Ziyang Zhang**,[1] **Shuai Yang**,[4] **and Ruiming Wang**[1]

[1]*State Key Laboratory of Biobased Material and Green Papermaking (LBMP), Qilu University of Technology, Jinan 250353, Shandong, China*
[2]*Key Laboratory of Industrial Fermentation Microbiology, Tianjin University of Science and Technology, Ministry of Education, Tianjin 300457, China*
[3]*Dongxiao Bioengineering (Shandong) Co., Ltd., Jinan 250000, Shandong, China*
[4]*Beijing Boxbio Science & Technology Co., Ltd., Beijing 101100, China*

Correspondence should be addressed to Ruiming Wang; ruiming3k@163.com

Received 5 May 2023; Revised 21 July 2023; Accepted 25 July 2023; Published 17 August 2023

Academic Editor: Seyed Mohammad Taghi Gharibzahedi

This study aimed at examining the structure-role modeling and antifatigue mechanism of polysaccharides, including *M. androsaceus* exopolysaccharide 3 (MEPS3), isolated from *Marasmius androsaceus* fermentation broth. The molecular weight of MEPS3 was 10.47 kDa. Furthermore, monosaccharide analysis showed the presence of mannose, glucose, and galactose in MEPS3 in a molar ratio of 0.08 : 0.34 : 1.46. Mannose, α-galactose, and α-d-glucose anomeric hydrogen signals were detected using nuclear magnetic resonance spectroscopy. MEPS3 was found to contain glyoxylic acid, forming rod-like chains that support high-purity polymerization. The weight-loaded swimming test results showed that MEPS3 treatment reduced lactic acid (LA) levels by 25.72% and increased the lactate dehydrogenase (LDH) activity by 5.67% in the plasma. Furthermore, it lowered malondialdehyde (MDA) levels by 47.09% and increased reactive oxygen species (ROS) and glutathione peroxidase (GSH-Px) levels by 52.42 and 97.03%, respectively, in the plasma. In addition, MEPS3 treatment reduced MDA and ROS levels in the liver by 28.85 and 18.64% while increasing superoxide dismutase (SOD) and GSH-Px levels by 17.41 and 38.13%, respectively. MEPS3 treatment increased the expression of nuclear factor-erythroid 2-related factor 2, glutamate-cysteine ligase, quinone oxidoreductase 1, and heme oxygenase 1 by 22.5, 24.8, 20.3, and 43.1%, respectively, in the liver. These findings demonstrate that MEPS3 effectively alleviates fatigue by removing harmful metabolites and indicate that the antifatigue mechanism is related to the Nrf-2 signaling pathway.

1. Introduction

Marasmius androsaceus, a well-known saprophytic mushroom, contains numerous components such as polysaccharides, proteins, mannitol, cholesterol acetate, amino acids, ergosterol, and hydroxycinnamic acid [1]. *M. androsaceus* possesses antihypertensive, antidepressant, antioxidant, analgesic, and immunomodulatory properties [2, 3]. Polysaccharides from the *M. androsaceus* broth are among the most important functional components. *M. androsaceus* polysaccharides have a high antidepressant activity and considerably increase norepinephrine and dopamine levels in mice. Western blot analysis revealed that *M. androsaceus* polysaccharides increase the expression of tyrosine hydroxylase, D2 dopamine receptor, and calcium-calmodulin-dependent protein kinase II.

Fatigue is characterized by a sense of tiredness that reduces the vitality and ability of an individual to perform daily activities. Although physical fatigue can be resolved by rest, dietary interventions, and medications [4], researchers are now turning their attention to natural products owing to their safety profile. Among these, polysaccharides have

gained increasing interest with regard to their structural characterization and the elucidation of mechanisms underlying their potential antifatigue effects [5].

The cause of fatigue is complex and variable. Fatigue is generally believed to be associated with energy metabolism, oxidative stress, and lipid peroxidation. Polysaccharides extracted from Codonopsis can substantially increase the glycogen content of the liver and muscle and reduce the blood urea nitrogen content in mice, thereby effectively relieving fatigue by increasing energy and reducing the accumulation of harmful metabolites [6]. Chi et al. [7] reported that polysaccharides isolated from Ziyang green tea can increase the activities of superoxide and GSH-Px and MDA content in the skeletal muscle and remarkably improve exercise-induced fatigue by reducing oxidative stress. Some studies have suggested that the antifatigue mechanism of okra polysaccharides involves a reduction in the accumulation of creatine kinase and lactate dehydrogenase in the serum and an increase in succinate dehydrogenase, adenosine triphosphate, and adenosine triphosphatase levels [8]. The antifatigue mechanism of the polysaccharide of *Spirulina platensis* may be related to increased hemoglobin levels; reduced lactic acid, urea nitrogen, and creatine kinase levels in the blood; inhibition of exercise-induced synthesis of 5-hydroxytryptamine and tryptophan hydroxylase expression; and increased serotonergic type 1 B inhibitory autoreceptor expression in the caudate putamen of exercised rats [9]. The antifatigue mechanism of *Polygonatum cyrtonema* Hua polysaccharide involves the regulation of osteocalcin signaling [10]. Research on antifatigue mechanisms is helpful for the development and utilization of natural antifatigue products. Recently, researchers have focused on the analgesic, antihypertensive, antioxidant, and antidepressant functions of *M. androsaceus* [11]. However, studies on the antifatigue effects of *M. androsaceus* polysaccharides are limited.

To study the antifatigue mechanism of *M. androsaceus*, a polysaccharide fraction, MEPS3, was purified. The structural characteristics were analyzed via molecular weight determination, monosaccharide composition analysis, and spectral and microscopic analyses. Moreover, the antifatigue activity of MEPS3 was investigated by evaluating animal behavior and the biochemical parameters associated with oxidative stress in fatigued mice; in addition, the antifatigue mechanism of MEPS3 was elucidated. Overall, this study aimed at identifying a new natural antifatigue product and providing experimental evidence to support the clinical use of MEPS3 as an effective antifatigue agent.

2. Materials and Methods

2.1. Materials and Reagents. The chemicals used in this study, including NaCl, $CHCl_3$, KH_2PO_4, $MgSO_4{\cdot}7H_2O$, vitamin B1, sucrose, peptone, yeast extract powder, trifluoroacetic acid, methanol, 1-phenyl-3-methyl-5-pyrazolone, potassium bromide, galacturonic acid, tetraborate, sulfuric acid, m-hydroxybiphenyl, D-mannose (Man), l-arabinose (Ara), fucose (Fuc), d-galactose (Gal), d-glucose (Glc), ribose (Rib), d-(Rha), and Rhodiola and radioimmunoprecipitation assay buffer, were obtained from Sigma-Aldrich (St. Louis, MO, USA). In addition, LA, LDH, ROS, SOD, GSH-Px, MDA, and protein assay kits were obtained from Beijing Boxbio Science & Technology Co., Ltd. (Beijing, China). Membrane and polyvinylidene fluoride membranes were obtained from Millipore (MA, USA). The primary antibodies against rabbit nuclear factor-erythroid 2-related factor 2 (Nrf-2) (code number: sc-81342), heme oxygenase 1 (HO-1) (code number: sc-390991), quinone oxidoreductase 1 (NQO1) (code number: sc-32793), and glyceraldehyde-3-phosphate dehydrogenase (GAPDH) (code number: sc-47724), and secondary horseradish peroxidase-labelled goat-anti-rabbit antibodies were purchased from Santa Cruz (California, USA). The primary antibodies against rabbit glutamate-cysteine ligase (GCLM) (code number: ab126704) were purchased from Abcam (Cambridge, UK).

2.2. Fermentation of Polysaccharides. M. androsaceus (CCTCC M2013175; China Center for Type Culture Collection, Wuhan, China) was cultured in a 100 L fully automatic fermenter (Biotech-100JS, BaoXing Bioscience Company, Shanghai, China) using a defined liquid medium containing 20 g/L sucrose, 10 g/L peptone, 10 g/L yeast extract powder, 1 g/L $MgSO_4{\cdot}7H_2O$, 1 g/L $KH_2PO_4{\cdot}3H_2O$, and 0.1 g/L vitamin B_1. The fermentation conditions were as follows: initial pH, 6.5; rotation speed, 300 rpm; culture duration, 6 days; culture temperature, 26°C; inoculum volume, 5%; ventilation volume, 200 L/h; inoculum age, 4 days; and loading volume, 70/100 L.

2.3. Extraction and Purification of Polysaccharides. In accordance with the conditions described in a previous study, we prepared the polysaccharides using a 6-day submerged fermentation and precipitation with ethyl alcohol. Extracellular polysaccharides, i.e., MEPS, were prepared by repeated protein removal, centrifugation, vacuum concentration, and freeze-drying. The separation of MEPS was accomplished using a DEAE-52 cellulose anion exchange column (2.6 cm × 35 cm) and a Sephadex G100 column (3.0 cm × 100 cm). We dissolved MEPS to a concentration of 10 mg/mL and conducted gradient separation on the DEAE-52 cellulose anion exchange column via elution with water, 0.1 M, 0.2 M, 0.3 M, and 0.4 M NaCl at a flow rate of 1 mL/min. We obtained the peaks of each component by merging, concentrating, dialyzing, and freeze-drying the eluates [11]. Subsequently, we collected and lyophilized three purified fractions, namely, MEPS1, MEPS2, and MEPS3 for further analysis.

2.4. Characterization of MEPS3

2.4.1. Ultraviolet (UV) Spectral Analysis and Purity Detection. MEPS3 was dissolved in distilled water at a concentration of 0.5 mg/mL. Full wavelength scanning was performed in the range of 200–400 nm using an ultraviolet-visible spectrophotometer (UV-mini 1240, Shimadzu Corp.,

Tokyo, Japan). The purity of MEPS3 samples was determined using a high-performance liquid chromatography (HPLC) system (1200, Agilent Technologies, California, USA) equipped with a TSK G4000 PWXL column (7.8 mm × 300 mm, 10 μm) and an RI-101 differential detector. The mobile phase was 0.9% NaCl, and the injection volume was 10 μL. The flow rate was 0.5 mL/min, and the temperature of the column compartment was controlled at 30°C. Before detection, MEPS3 was dissolved in deionized water and then filtered through a membrane with 0.22 μm diameter to remove impurities [11].

2.4.2. Determination of Molecular Weight. An HPLC-refractive index detector (RID) (1260 RID, Agilent Technologies, California, USA) equipped with a TSK-G 5000WXL (7.8 mm × 300 mm) was used to analyze the molecular weight. The fractions (1 mg/mL) were dissolved in distilled water and filtered using 0.45 μm filters. The analysis conditions were as follows: water at a flow rate of 0.6 mL·min^{-1} was used for elution, and 20 μL of the solution was injected in each run at a column and detector temperature of 25°C. The molecular weights of the polysaccharide fractions were estimated using a calibration curve prepared using a series of dextran standards (2000, 500, 70, 40, and 10 kDa) [11].

2.4.3. Determination of Monosaccharide Composition. The monosaccharide composition of MEPS3 was determined as described in our previous method [11]. In brief, a 2 mg polysaccharide sample was hydrolyzed with 2 M trifluoroacetic acid (2 mL) at 120°C for 3 h in a sealed ampoule bottle. Subsequently, the hydrolysate was distilled under a vacuum using methanol and nitrogen to remove excess acid. Finally, the dried hydrolytic sample was derivatized in a sealed ampoule with a 2 mol/L 1-phenyl-3-methyl-5-pyrazolone (PMP)-methanol solution (100 μL) at 70°C for 30 min. The products were centrifuged at 8000 rpm for 5 min, and the supernatant was mixed with 0.3 M HCl (100 μL). Excess PMP was removed using $CHCl_3$, and centrifugation at 8000 rpm for 2 min was performed to remove $CHCl_3$. The derivatives were analyzed using an HPLC-UV system, equipped with a Zorbax SB-C18 column (150 × 4.6 mm, 5.0 m), and detected at 250 nm. The mobile phase consisted of 0.05 M KH_2PO_4 (pH 6.7) with 83 (solvent *A*) and 17% (solvent *B*) acetonitrile at a flow rate of 1 mL/min. The injection volume used was 20 μL.

2.4.4. Determination of Uronic Acid Content. The uronic acid in MEPS3 was analyzed using the m-hydroxybiphenyl method [12]. In brief, 1 mL aliquots of a series of gradients of galacturonic acid were precooled in an ice water bath. Then, 1.5 mL sodium tetraborate and sulfuric acid were added to the mixture and placed in a boiling water bath for 5 min. After cooling, 25 μL of m-hydroxybiphenyl was added. The absorbance was measured at 520 nm, and a standard curve was drawn. The polysaccharide sample (10 mg) was hydrolyzed to 10 mL. The prepared polysaccharide sample was added to 1 mL to determine the uronic acid content of the polysaccharide according to the abovementioned method.

2.4.5. Fourier Transform Infrared (FT-IR) Spectroscopy Spectral Analysis. The purified fractions were mixed with dried potassium bromide powder (1 : 150) and pressed into a 1 mm wafer for FT-IR measurement. The corresponding spectra were recorded using an FT-IR spectrophotometer (Nicolet 6700, Thermo Electron Corp., Waltham, MA, USA) within the frequency range of 4000–400 cm^{-1} [13].

2.4.6. Nuclear Magnetic Resonance (NMR). MEPS3 was dissolved in heavy water (supersaturated solution) to record ^{1}hydrogen (64 scans) and ^{13}carbon (15k scans) NMR spectra (with a BBFO-plus probe) on a Bruker spectrometer (AV-400, Bruker Daltonics Inc., MA, USA) at 30°C and 600 MHz [14].

2.4.7. Scanning Electron Microscopy (SEM). The morphological characteristics of MEPS3 were observed using SEM (JSM-7500, JEOL, Japan). The vacuum-dried sample was placed on a specimen holder with Al and sputtered with Au powder using a vacuum-coating apparatus at an accelerating voltage of 5 kV and image magnification of 800x [15].

2.4.8. Atomic Force Microscopy (AFM). MEPS3 was diluted to a concentration of 5 μg/mL with distilled water and filtered through a 0.45 μm filter (NYL, 13 mm syringe filter, Whatman, Inc., Piscataway, NJ, USA). A drop of MEPS3 solution was placed on freshly cleaved mica, dried at room temperature, and observed using a digital instrument (Multi Mode 8; Bruker Daltonics Inc., Billerica, MA, USA) [16].

2.5. Animals and Treatments. Male Kunming mice (5 weeks old, 18–20 g) were purchased from Vital River Laboratory Animal Technology Co., Ltd. (Beijing, China). The mice were kept in a controlled environment with a 12 h light/black cycle and a temperature of 22 ± 2°C. Food and water were provided *ad libitum*. After 1 week of adaptation, the mice were randomly divided into four groups (n = 7/group) on the basis of different concentrations of MEPS dissolved in distilled water fed to them. The groups were as follows: control (distilled water), MEPS1 (180 mg/kg, i. g.), MEPS2 (60 mg/kg, i. g.), and MEPS3 (30 mg/kg, i. g.) groups. The treatments were administered intragastrically for 14 days. One-hour posttreatment, antifatigue ability tests were conducted. Based on animal behavior tests, polysaccharide fractions with a high antifatigue activity were screened for use in subsequent animal experiments and structural characterization [17].

Another set of male Kunming mice was randomly divided into eight groups (n = 7/group), namely, the vehicle (administered distilled water), which was further subdivided into native and control; two Pro (administered Rhodiola, 300 mg/kg); two LD (administered a low dose of MEPS3, 30 mg/kg, i. g.); and two HD (administered a high dose of

MEPS3, 300 mg/kg, i. g.) groups. The treatments were administered intragastrically for 14 days. After the last intragastric administration, the mice in the control, Pro, LD, and HD groups were forced to swim for 10 min to establish a fatigue model. All animal procedures were performed in accordance with the Guidelines for Care and Use of Laboratory Animals (Ministry of Science and Technology of China, 2006) and were approved by the Institutional Animal Committee of Qilu University of Technology (QLU20200625).

2.6. Fatigue Tolerance Test

2.6.1. Electric Tolerance Test. The animals in the different groups were trained three times before the last administration. The mice in each group were placed on a Plexiglass rod such that their muscles were in a static-tension state. We set the speed at 10 r/min. After training, the mice in each group were intragastrically treated for 30 min after the last administration of the test samples and placed on a Plexiglass rod (ZB-200, Taimeng Technology Co., LTD., Chengdu, China); the rotation speed was set at 20 rpm. The rotarod times of the mice falling from a glass rod due to muscle fatigue were recorded three times in parallel [18].

2.6.2. Rotarod Time Test. Adaptability training was performed in different groups before the last administration of the test samples. Mice in each group were placed on a treadmill (804, Yuyan Scientific Instrument Co., LTD., Shanghai, China) at a speed of 20 rpm, and the current was adjusted to the highest level so that they could understand how to escape the charged area. Thirty minutes later, the mice in each group were placed on a treadmill, with the speed set at 30 rpm. The duration of the electric shock for 5 min was recorded three times in parallel [18].

2.6.3. Weight-Loaded Swimming Test. The weight-loaded swimming test was performed based on a previous study, with some modifications. The mice were forced to swim without loading for 10 min before the experiment to allow them to acclimatize to swimming. One hour after the last administration of the test samples, the weight-loaded swimming test was used. The mice were placed in an open cylindrical container (80 cm × 40 cm), which contained fresh water maintained at 22 ± 1°C and was approximately 35 cm deep such that the animal failed to touch its bottom. A lead weighing approximately 5% of the body weight of the mice was attached to the tail. Exhaustion was determined by observing the loss of coordinated movements and failure to return to the surface within 10 s, and exhaustive swimming time was recorded immediately [10, 19, 20].

2.7. Sample Collection and Measurement. Blood was collected from the orbital venous plexus of the mice of each group before and after the weight-loaded swimming test. Plasma sample was prepared by centrifugation at 4000 rpm and 4°C for 10 min and stored at −80°C. The mice were sacrificed by cervical vertebra dislocation, and their livers were collected and stored at −80°C. The levels of LA, LDH, ROS, SOD, GSH-Px, MDA, and tissue proteins were determined using commercially available kits in accordance with the manufacturer's protocol.

2.8. Western Blotting. A portion of the collected liver samples was homogenized in radioimmunoprecipitation assay buffer containing a 1% protease inhibitor cocktail. Protein concentrations were determined using a bicinchoninic acid kit and adjusted to the same level as that of the 5x loading buffer. Proteins (10 μL) were separated using 10% sodium dodecyl sulfate-polyacrylamide gel electrophoresis (spacer gel, 80 V; separation gel, 120 V) and transferred onto polyvinylidene fluoride membranes. The membranes were blotted with primary antibodies against Nrf-2 (1 : 1000), HO-1 (1 : 1000), NQO1 (1 : 1000), GCLM (1 : 1000), and GAPDH (1 : 1000) at 4°C overnight, followed by incubation with horseradish peroxidase-conjugated secondary antibodies (1 : 1000) for 1 h. Chemiluminescence was detected using an infrared laser imaging system (Odyssey, LI-COR Inc., USA) [21]. Western blot bands were quantified using ImageJ (version 1.8.0, Bethesda Software LLC, MD, USA).

2.9. Statistical Analysis. Each experiment was performed independently in triplicate. The results are expressed as the mean ± standard deviation (mean ± SD). The Kolmogorov–Smirnov (K-S) test was used to verify the normality of data distribution and to confirm that the data were within the normal range. Data were analyzed using a one-way analysis of variance and Tukey's multiple comparison tests using the SPSS software (SPSS 16.0 for Windows, SPSS Inc., Chicago, IL, USA). Origin 8.5 (version 8.5, OriginLab Corporation, Northampton, USA) was used to illustrate the figures, and the statistical significance was set at $P < 0.05$.

3. Results and Discussion

3.1. Extraction, Purification, and the Antifatigue Activity of Polysaccharide Fractions. Crude MEPS was isolated from *M. androsaceus* through fermentation and separated via gradient elution using DEAE-52 cellulose anion-exchange column chromatography with 0, 0.1, 0.2, 0.3, 0.4, and 0.5 M NaCl solutions. We found (Figure 1(a)) that MEPS was eluted in three fractions, namely, MEPS1, MEPS2, and MEPS3. These fractions were concentrated under a vacuum, dialyzed against distilled water, and lyophilized, and the relevant components were collected. The polysaccharide content was quantified using the phenol-sulfuric acid method; results showed that the MEPS1, MEPS2, and MEPS3 content ratios were 6 : 2 : 1.

The antifatigue properties of MEPS1, MEPS2, and MEPS3 were evaluated through animal behavior experiments, including the electric shock, rotarod, and weight-loaded swimming time tests, to screen for a favorable antifatigue effect of the test compounds (Figure 2). Intragastric concentrations were set according to the content ratios of MEPS1, MEPS2, and MEPS3. Results showed that the three

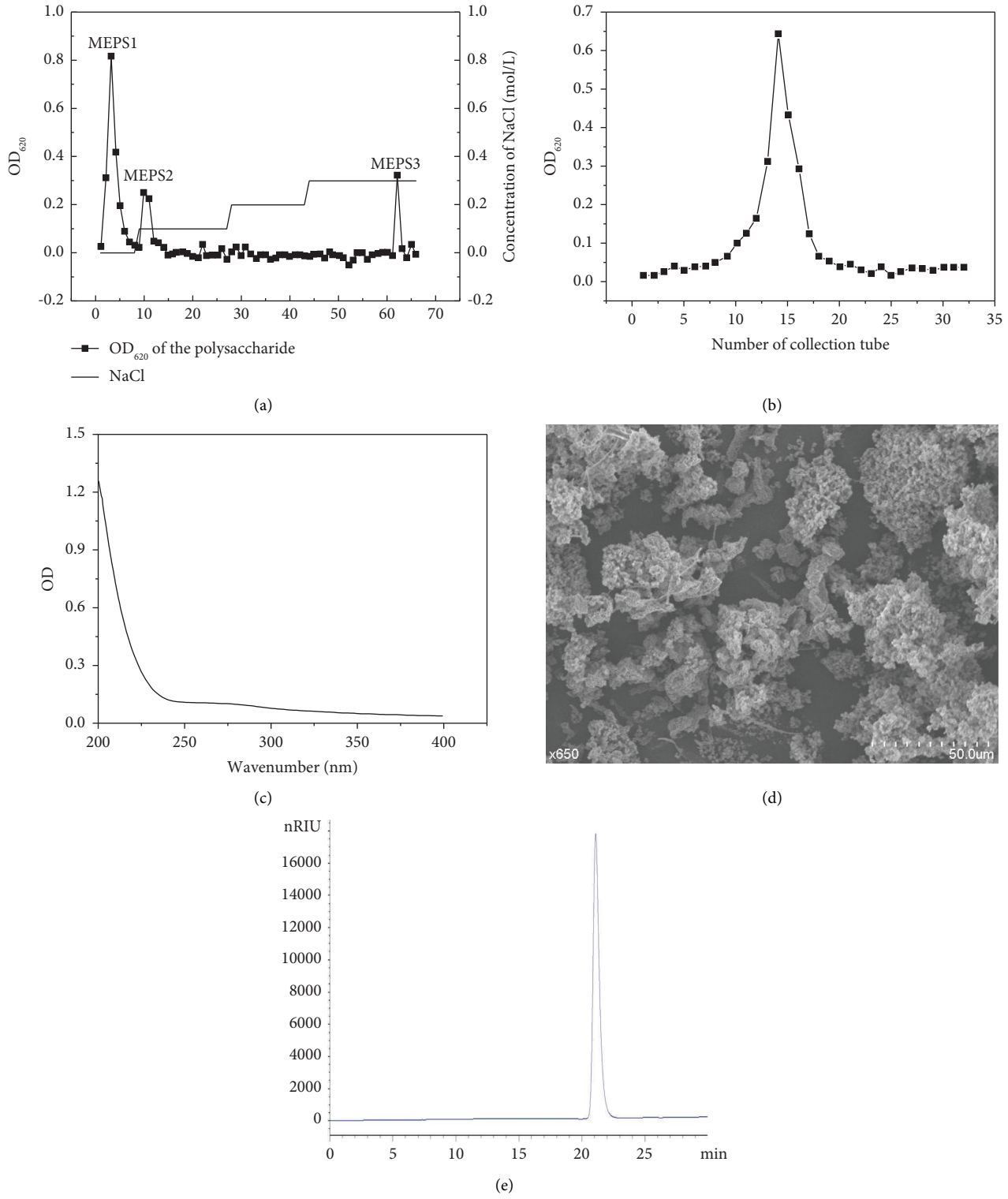

Figure 1: (a) Fractionation of *Marasmius androsaceus* polysaccharides using DEAE-52 chromatography. (b) MEPS3 was further separated by Sephadex G-100 column chromatography, and (c) the UV spectra, (d) micrographs, and (e) purity of MEPS3 were examined.

fractions exerted different degrees of antifatigue effects. Specifically, after 14 days of treatment with the three fractions, MEPS1 (180 mg/kg) increased the time spent on the rotarod apparatus and weight-loaded swimming by 32.8 and 45.4%, respectively, without changing the electric shock time. MEPS2 (60 mg/kg) treatment had no significant effect on the electric shock, rotarod, and swimming times. However, MEPS3 (30 mg/kg) treatment significantly increased the rotarod and swimming times by 38.9 and 49.2%, respectively ($P < 0.05$) and decreased the electric shock time

by 48.05% compared with those in the vehicle group ($P < 0.05$). These results indicated that MEPS3 had the highest antifatigue capacity. Our results are in tandem with an antifatigue study of okra polysaccharides; the crude polysaccharides extracted from okra (*Abelmoschus esculentus* (*L.*) *Moench*) effectively prolonged the swimming time of mice in a weight-bearing swimming experiment [20]. In an antifatigue study of *Polygonatum cyrtonema* Hua polysaccharide, we observed a significant increase in the exhaustive swimming time of mice compared to that in the normal control group [10]. Similarly, in the investigation of *Cordyceps militaris* acidic polysaccharides (CMPB), mice gavaged with CMPB had considerably longer stick rotation times in the rotarod test than those in the model group, which suggested enhanced exercise endurance [22]. Previous research has highlighted *Ganoderma lucidum* as an antifatigue food, with *Ganoderma lucidum polysaccharide* (*GLPs*) identified as its main antifatigue component [23]. In the forced swimming test, mice gavaged with GLPs exhibited considerable antifatigue activity [24]. These substantial lines of evidence indicate that polysaccharides potentially have antifatigue properties. Therefore, we performed the structural characterization of MEPS3 and used it in animal experiments to determine its antifatigue mechanism [25].

3.2. Characterization of MEPS3

3.2.1. UV Spectrum and Purity Analyses of MEPS3. MEPS3 exhibited no absorption peaks at 260 or 280 nm in the UV spectrum (Figure 1(c)), which indicated the absence of nucleic acids and proteins. Subsequently, the MEPS3 fraction was purified using Sephadex-G100 dextran gel column chromatography (Figure 1(b)). The purity of the purified polysaccharide sample, i.e., MEPS3, was determined via HPLC (Figure 1(e)). After MEPS3 passed through the gel column, a single and symmetrical chromatographic peak was obtained, and the peak emergence time was 21.09 min. The peak area was 96%, indicating that MEPS3 was a homogeneous component. In addition, the purity of MEPS3, as determined using the phenol-sulfuric acid method, was 96.12%.

3.2.2. Molecular Weight of MEPS3. The biological activity of polysaccharides is related to their molecular weights [26]. The molecular weight was determined using HPLC-RID with TSK-G5000WXL (7.8 mm × 300 mm) and a calibration curve of dextran standards ($\log Mw = -0.1864t + 7.9977$; $R^2 = 0.99704$) obtained using HPLC [11]. The peak time for MEPS3 was 21.087 min. Based on the calibration with standard dextran, the estimated molecular weight was 10.47 kDa (Figure 3(a)).

3.2.3. Monosaccharide Composition of MEPS3. MEPS3 contains mannose, glucose, and galactose in a molar ratio of 0.08 : 0.34 : 1.46, which indicates that MEPS3 is a heteroglycan (Figure 3(b)). In the previous studies, polysaccharides from *Cordyceps sinensis*, a valuable medicinal material with antifatigue effects, had monosaccharide composition and molar ratios similar to those of MEPS3, which suggests that MEPS3 may have antifatigue effects [27].

The high galactose content of acidic polysaccharides accounts for their antifatigue activity [28]. Maca polysaccharides, which contain D-GalA : D-Glc : L-Ara : D-Man: D-Gal : L-Rha in a ratio of 35.07 : 29.98 : 16.98 : 13.01 : 4.21 : 0.75, are acidic polysaccharides with a high D-GalA content and good antifatigue effects. The mannose content of polysaccharides contributes to their biological activities, including antifatigue, antitumor, and immunostimulatory effects [29, 30]. The antifatigue effects of MEPS3 might be related to its mannose content.

3.2.4. Determination of Uronic Acid Content. Galacturonic acid was used as the standard, and the galacturonic acid content, which was in the range of 10–200 μg/mL, showed a good linear relationship with the absorbance. The uronic acid content in MEPS3 was 4.2% according to the standard curve ($Y = 0.00875X + 0.01306$; $R^2 = 0.996$). Polysaccharides with biological activities are mostly acidic. In a previous study, the polysaccharides extracted from four berries used in traditional medicinal foods (*Tibetans Hippophae rhamnoides* L., *Lycium barbarum* L., *Lycium ruthenicum* Murr., and *Nitraria tangutorum* Bobr.) containing uronic acids were found to be effective in resolving the fatigue caused by hypoxia [31].

3.2.5. FT-IR Analysis of MEPS3. The infrared spectrum of MEPS3 is shown in Figure S1. A strong and wide stretching peak, which was caused by the stretching vibration of O-H, was observed at 3423 cm^{-1} and is a typical carbohydrate peak. A wider peak also indicates a weak hydrogen bond between the hydroxyl groups [32, 33]. In addition, several weak peaks at approximately 2926 cm^{-1} caused by the -OH and C-H stretching vibrations exist [34]. The absorption peak near 1623 cm^{-1} was attributed to the antisymmetric stretching vibrations of carboxylate anions (COO-), confirming the presence of uronic acid [35]. The stretching vibration of the absorption peak C-O-H and the vibration of the C-O-C glycoside bond in the range of 1200–1000 cm^{-1} are related, which indicates the presence of a pyranose ring in MEPS3 [36]. In addition, a weak band near 807 cm^{-1} indicates the presence of β-chain glycosyl residues [37].

3.2.6. NMR Analysis of MEPS3. The H spectrum of MEPS3 (Figure 4(a)) showed that the H atom signals between 4.9 and 4.3 ppm were assigned to anomeric protons of β-anomers, while the signals above 5.0 ppm were assigned to anomeric protons of α-anomers, indicating that mainly α-glycosidic linkages are present in the backbone [38, 39]. No proton signal occurred at 5.4 ppm, indicating that GF was composed of pyranose [30], which is consistent with the FT-IR analysis results. Generally, signals between 1.1 and 1.3 ppm indicate the presence of the 6-deoxy sugar methyl doublet [39]. The chemical shift signals in the 1.79–2.23 ppm region indicate the presence of acetyl groups and methyl

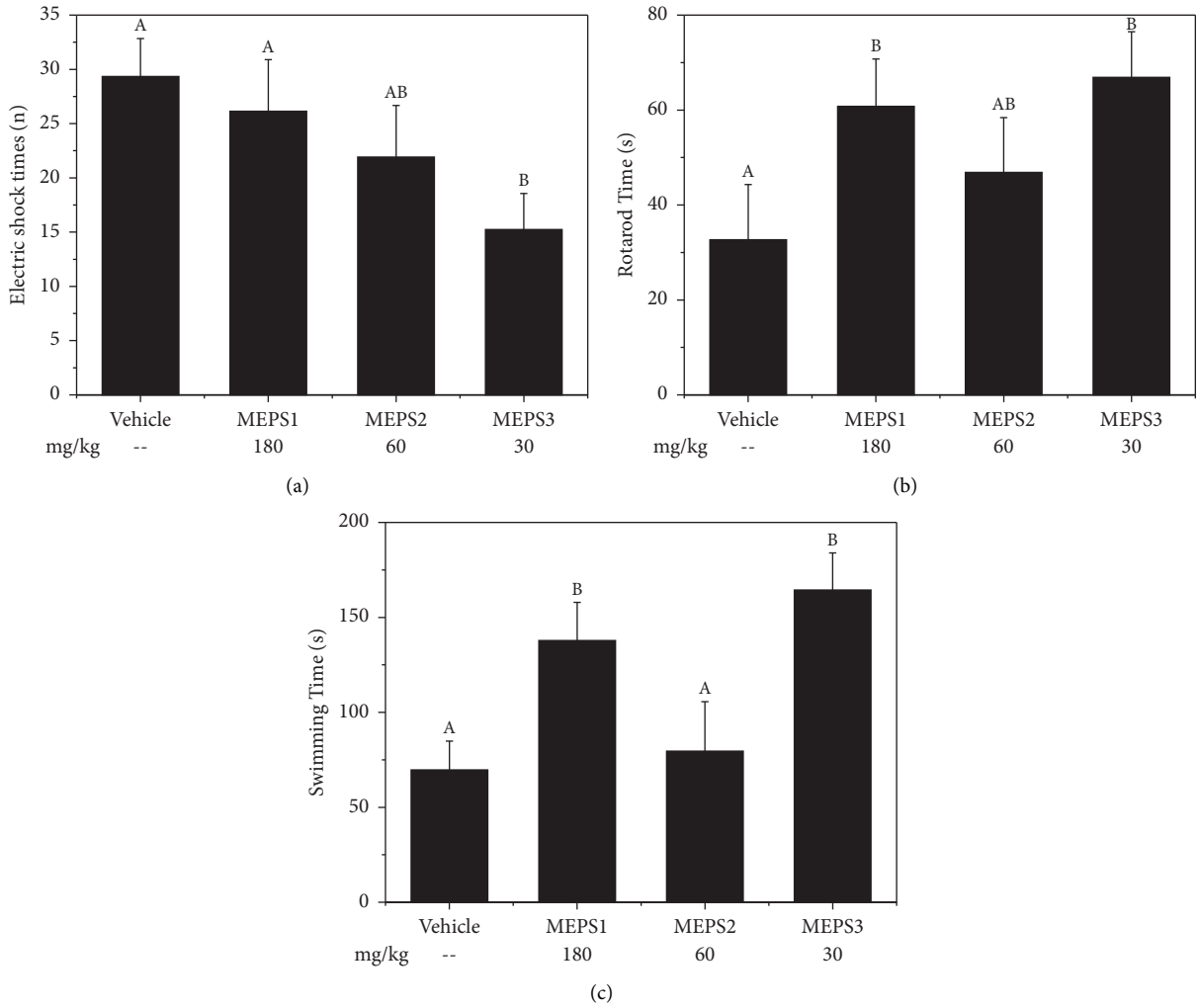

Figure 2: Effects of MEPS treatment on (a) electric shock times, (b) rotarod time, and (c) swimming time in exercise endurance tests. Data are expressed as the mean ± SD. (A, B) Bars with different superscripts are significantly different ($P < 0.05$).

esterification carboxyl groups, which to some extent indicates that MEPS3 contains uronic acid [40]. Owing to the presence of methyl or methylene protons near the double bonds or carbonyl groups, the ^{1}H NMR spectrum of MEPS3 exhibited a prominent signal in the range of 3.50–4.11 ppm, which may be attributed to the CH2-O and CH-O groups of sugars [30, 41, 42]. In addition, signals in the range of 5.12–4.90 ppm for the glucuronic acid residues of MEPS3 were visible [43]. The characteristic peak of mannose was δ4.787 ppm. The signals in δ5.062, 5.107, and 5.159 were α-galactose signals, and the signals in δ5.313 were α-D-glucose anomeric hydrogen signals [44], which is consistent with the results of monosaccharide composition. The ^{13}C NMR spectrum of the polysaccharide (Figure 4(b)) showed a regular structure. The β-anomeric carbon signal appeared at δ102.23 ppm in the C spectrum of the polysaccharide, which may belong to (1 ⟶ 4)-α-Manp [45]. The peak at δ23.32 ppm was the acetyl-methyl carbon signal peak. The characteristic signals that appeared at δ102.60–104.46 ppm in the C spectrum of the polysaccharide were assigned to the $C-1$ of Galp. The signals of the ring carbons appeared in the region between δ65.12 and 82.13 ppm [46]. The absence of signals in the δ82–88 region confirmed the pyranose form of all sugar residues [47], which is consistent with the results of ^{1}H NMR analysis. The main proton and carbon signals are listed in Table S1.

3.2.7. SEM Analysis of MEPS3. As shown in Figure 1(d), the SEM micrographs of MEPS3 revealed the surface morphology of the polysaccharide. SEM images (800x magnification) showed that MEPS3 had a high degree of heterogeneity, with spherical particles, rod-shaped structures of different sizes, and cross-linkages between them.

3.2.8. AFM Analysis of MEPS3. A topographical AFM planar image of 5 μg/mL MEPS3 is shown in Figure 5(a), where individual molecules can be observed within the dilute regions. The irregular and spherical lumps are shown in Figures 5(a) and 5(b), respectively. Occasionally, a stick-type lump attributed to the entanglement of multiple molecular chains was observed. The diameter and height of the

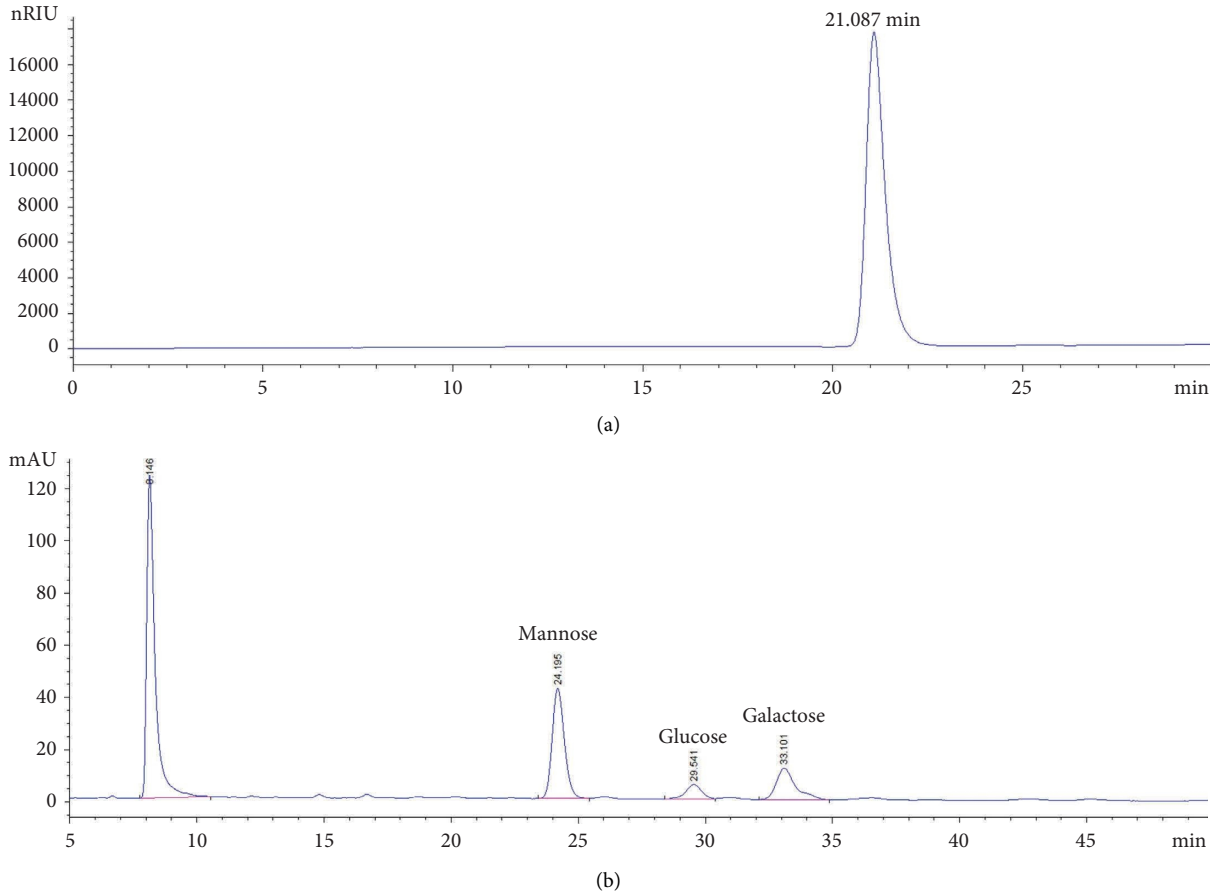

Figure 3: (a) Gel permeation chromatogram of the MEPS3 solution and (b) HPLC chromatogram of the MEPS3 hydrolysate.

lumps were 10–200 and 5–31 nm, respectively. The height and width of the molecules varied according to the measurement position.

3.2.9. Effect of MEPS3 Treatment on Body Weight. Body weights were recorded weekly (Table 1). No significant differences in body weights were observed between the vehicle and treatment groups. The results suggested that MEPS3 (30 and 300 mg/kg) and Rhodiola (300 mg/kg) had no significant effect on mouse body weights when compared with those in the vehicle group.

3.2.10. Effects of MEPS3 on LA Levels and LDH Activity in the Plasma. LA levels and LDH activity in the plasma were determined after 2 weeks of intragastric administration, in accordance with the manufacturer's instructions. Before the weight-loaded swimming experiment, no significant differences were observed in the plasma LA levels between the vehicle and treatment groups (Figure 6(a)). Fatigue is a complex metabolic state characterized by the accumulation of LA and carbon dioxide [20, 25]. LA is the product of energy metabolism. Excessive LA production can decrease the pH and inhibit muscle contraction. Therefore, eliminating LA promptly is beneficial in relieving fatigue. The weight-loaded swimming test was conducted to build a fatigue model; the LA content in mice was found to be significantly increased. The increase in the LA content caused by fatigue reduced after the intragastric administration of MEPS3 and Pro. Furthermore, the plasma LA levels of the HD and Pro groups decreased by 25.72 and 22.18%, respectively, and the HD group showed a better antifatigue effect than the Pro group. With an increase in MEPS3 intragastric dose, the decrease in LA was more evident, showing a dose-dependent relationship.

LDH normally exists in muscle cells; however, it is released into the blood when the muscle is damaged [48]. Thus, an increase in plasma LDH levels is indicative of tissue damage and fatigue. After weight-loaded swimming, the LDH activity in the vehicle group showed no statistical difference from that before weight-loaded swimming. However, compared with the vehicle group, the MEPS3 dose and Pro groups showed improved LDH activity in mouse plasma; the HD group showed the most obvious effect, with the LDH activity increasing by 5.67% (Figure 6(b)). Maca polysaccharides exert antifatigue effects by reducing LA and LDH levels in mouse serum [28]. In this study, in the MEPS3 group, the plasma LA levels decreased and the plasma LDH activity increased in a dose-dependent manner compared to those in the vehicle group (Figures 6(a) and 6(b)). These

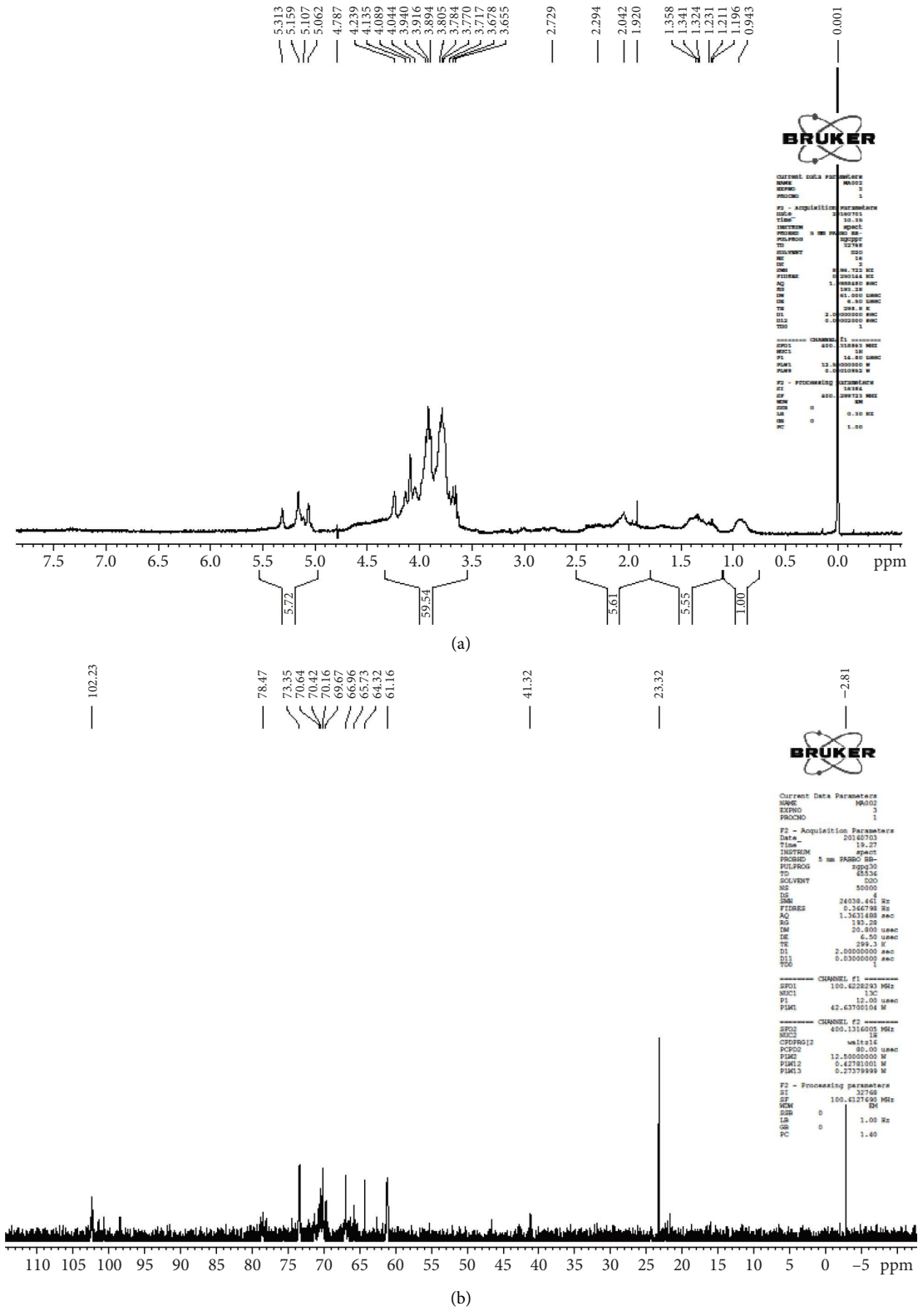

Figure 4: NMR spectra of MEPS3: (a) ^{1}H NMR spectrum and (b) ^{13}C NMR (DEPT-135) spectrum.

results indicated that MEPS3 supplementation improved endurance capacity because of the rapid removal of harmful metabolites in swimming experiments.

3.2.11. Effects of MEPS3 on Liver ROS Levels. Fatigue is associated with oxidative stress. Generally, oxidative stress is induced by the overgeneration of ROS, and fatigue leads to

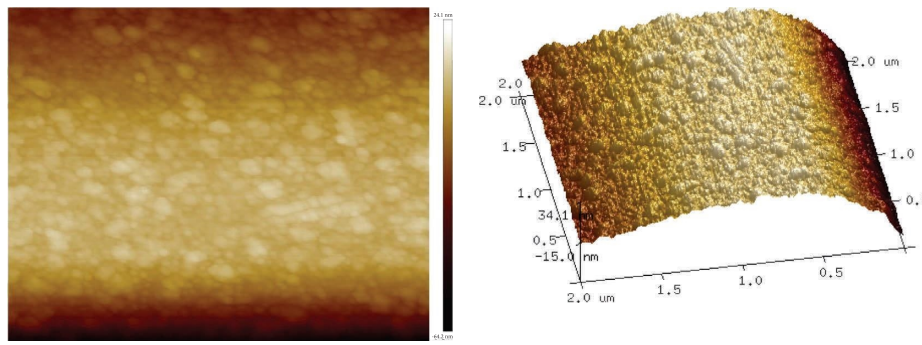

(a) (b)

Figure 5: AFM micrographs of MEPS3: (a) planar view and (b) cubic view.

Table 1: Effects of Rhodiola (300 mg/kg, oral gavage (i.g.)) and MEPS3 (30 and 300 mg/kg, i.g.) treatments on mouse body weight.

Groups	Initial	Intermediate	Terminal
Vehicle	20.5 ± 0.8^a	22.6 ± 1.3^a	24.5 ± 1.2^a
Pro (s)	20.4 ± 1.0^a	22.7 ± 1.5^a	24.9 ± 1.4^a
LD (s)	20.6 ± 0.7^a	22.9 ± 0.9^a	25.0 ± 1.5^a
HD (s)	20.4 ± 1.2^a	22.4 ± 1.2^a	24.3 ± 1.3^a

Data are expressed as the mean ± SD. Values in the same row with the same letters are not significantly different ($P > 0.05$). Pro, administered Rhodiola; LD, administered a low dose of MEPS3; and HD, administered a high dose of MEPS3.

excessive ROS production during exhaustive exercise, which indicates that ROS is a major indicator of physical fatigue [49]. The concentration of ROS in the liver was evaluated two weeks after the intragastric administration. The results demonstrated that the liver ROS content was similar to that of the vehicle group in each treatment group before the weight-loaded swimming test. However, after weight-loaded swimming, the ROS content in the vehicle group was significantly ($P < 0.05$) higher than that before swimming; it is possible that the ROS content increased because fatigue was alleviated upon gavage with Pro or MEPS3. Compared with those in the vehicle group, the ROS levels in the livers of the Pro, LD, and HD groups decreased by 19.18, 11.95, and 18.64%, respectively, which indicated that MEPS3 can scavenge ROS in a dose-dependent manner and that the antifatigue ability of MEPS3 may be involved in the antioxidant system (Figure 6(c)).

3.2.12. Effects of MEPS3 on Oxidative Stress and Antioxidant Biomarker Levels in the Plasma and Liver. We measured MDA, SOD, and GSH-Px levels in the plasma and livers of mice before and after weight-loaded swimming and further explored the association between MEPS3 and antifatigue (Tables 2 and 3). The results showed that after weight-loaded swimming, in the group with high dose of MEPS3, the MDA content decreased by 47.09% and SOD and GSP-Px levels increased by 52.42 and 97.03%, respectively, in the plasma, whereas the levels of MDA decreased by 28.85%, and the GSH-Px and SOD levels in the liver increased by 38.13 and 17.41%, respectively. During exercise, the body experiences oxidative stress, which disrupts the oxidation system and causes the generation of numerous free radicals, leading to cellular and tissue damage. Unsaturated fatty acids are attacked by excessive oxygen free radicals to produce lipid peroxides. MDA is the final metabolite of lipid peroxides, and its content is proportional to the damage to cells caused by oxygen free radicals [19, 50]. In addition, SOD and GSP-Px can clear superoxide anion free radicals from the body and play a role in resolving fatigue. During exercise, because of the large amount of glucose consumed, liver cells can decompose liver glycogen into glucose during blood circulation [51]. Therefore, the activities of SOD and GSP-Px in the livers of the blank group increased, whereas the levels of SOD and GSP-Px in the plasma decreased after weight-loaded swimming, indicating that oxidative stress is closely related to fatigue.

In this study, compared to that in the vehicle group, a high dose of intragastrically administered MEPS3 reduced the MDA content in the plasma and livers of mice after weight-loaded swimming, increased SOD and GSP-Px activities, and played a positive role in scavenging the free radicals generated by fatigue. Overall, MEPS3 supplementation significantly reduced MDA and ROS levels and increased antioxidative enzyme levels (SOD and GSP-Px), which suggests that MEPS3 protects the cells from oxygen free radical damage, prevents biofilm-mediated damage, and exerts antifatigue effects by modulating oxidative stress.

3.2.13. Effects of MEPS3 on the Expression of Key Proteins Involved in Nrf-2 Signaling. The Nrf-2/antioxidant response element (ARE) pathway plays an important role in regulating oxidative stress [52]. The expression of the Nrf-2 and Nrf-2 downstream key proteins HO-1, NQO1, and GCLM was evaluated via western blotting of the livers of weight-loaded swimming mice (Figure 7). Results revealed that the expression of Nrf-2 and its downstream proteins in the livers of mice in the control group was significantly higher than that in the native group. However, MEPS3 treatment, especially in the HD group, significantly increased the expression of Nrf-2, GCLM, NQO1, and HO-1 in the liver by 22.5, 24.8, 20.3, and 43.1%, respectively. These results demonstrated that swimming downregulates the key proteins involved in Nrf-2 signaling, whereas MEPS3 upregulates them.

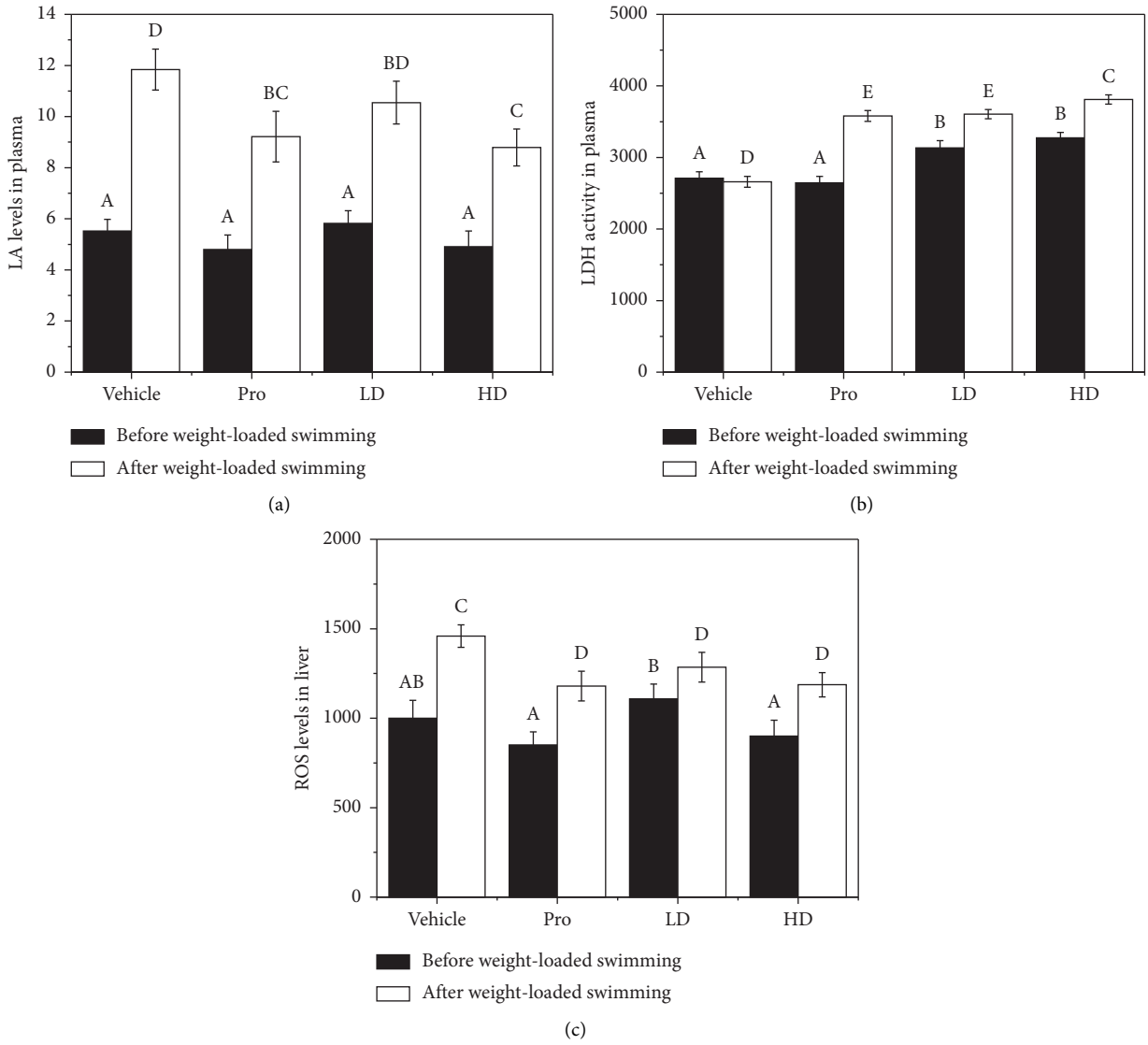

Figure 6: Effects of Rhodiola (300 mg/kg, i.g.) and MEPS3 (30 and 300 mg/kg, i.g.) treatments on (a) plasma LA levels, (b) plasma LDH activity, and (c) liver ROS levels. Data are expressed as the mean ± S.D. (A–E) Bars with different superscripts are significantly different ($P < 0.05$). Pro, administered Rhodiola; LD, administered a low dose of MEPS3; and HD, administered a high dose of MEPS3.

Table 2: Effects of Rhodiola (300 mg/kg, i.g.) and MEPS3 (30 and 300 mg/kg) treatments on oxidative stress and antioxidant biomarker levels in the mouse plasma.

Groups	Indicator	Vehicle	Pro (mg/kg)	MEPS3 (mg/kg)	
			300	30	300
Before test	MDA (nmol/mL)	17.79 ± 0.51^{a}	11.87 ± 0.28^{b}	15.60 ± 0.57^{c}	10.13 ± 0.41^{d}
	SOD (U/mL)	82.87 ± 2.71^{a}	71.37 ± 2.48^{b}	87.49 ± 2.95^{ac}	90.64 ± 2.69^{c}
	GSH-Px (μmol/mL)	94.89 ± 2.85^{a}	94.24 ± 2.37^{a}	95.19 ± 2.42^{a}	97.05 ± 3.95^{a}
After test	MDA (nmol/mL)	20.96 ± 0.45^{a}	11.21 ± 0.42^{c}	15.82 ± 0.34^{b}	11.09 ± 0.29^{c}
	SOD (U/mL)	66.93 ± 1.88^{a}	93.43 ± 1.95^{b}	88.03 ± 2.62^{c}	102.02 ± 2.52^{d}
	GSH-Px (μmol/mL)	80.22 ± 1.93^{a}	157.88 ± 3.62^{c}	121.78 ± 3.64^{b}	158.06 ± 4.15^{c}

Data are expressed as the mean ± SD. Values in the same row with different letters (a, b, c, and d) are significantly different ($P < 0.05$).

Nrf-2 is the central transcriptional regulator of ARE-driven gene expression in response to oxidative stress. Under oxidative stress, Nrf-2 is translocated from the cytoplasm into the nucleus to activate the expression of antioxidant enzymes such as SOD and GSH-Px. When the Nrf-2/ARE pathway is activated, the induction of GCLM, HO-1, and NQO1 expression by polychlorinated biphenyl quinone plays an important role in adaptation to oxidative stress [52].

Table 3: Effects of Rhodiola (300 mg/kg, i.g.) and MEPS3 (30 and 300 mg/kg, i.g.) treatments on oxidative stress and antioxidant biomarker levels in the mouse liver.

Groups	Indicator	Vehicle	Pro (mg/kg)	MEPS3 (mg/kg)	
			300	30	300
Before test	MDA (nmol/mL)	9.56 ± 0.17^{a}	9.20 ± 0.32^{a}	7.75 ± 0.45^{b}	7.46 ± 0.46^{b}
	SOD (U/mL)	96.81 ± 1.10^{a}	103.84 ± 1.10^{b}	92.33 ± 0.38^{c}	98.84 ± 0.67^{d}
	GSH-Px (μmol/mL)	20.74 ± 0.57^{a}	21.57 ± 0.30^{ab}	22.71 ± 0.72^{b}	24.52 ± 0.89^{c}
After test	MDA (nmol/mL)	12.48 ± 0.16^{a}	7.81 ± 0.40^{b}	9.48 ± 0.46^{c}	8.88 ± 0.24^{c}
	SOD (U/mL)	118.66 ± 2.42^{a}	154.56 ± 2.37^{b}	128.08 ± 1.63^{c}	163.91 ± 2.27^{d}
	GSH-Px (μmol/mL)	24.12 ± 0.22^{a}	28.43 ± 0.40^{b}	26.36 ± 0.34^{c}	28.32 ± 0.27^{b}

Data are expressed as the mean ± SD. Values in the same row with different letters (a, b, c, and d) are significantly different ($P < 0.05$).

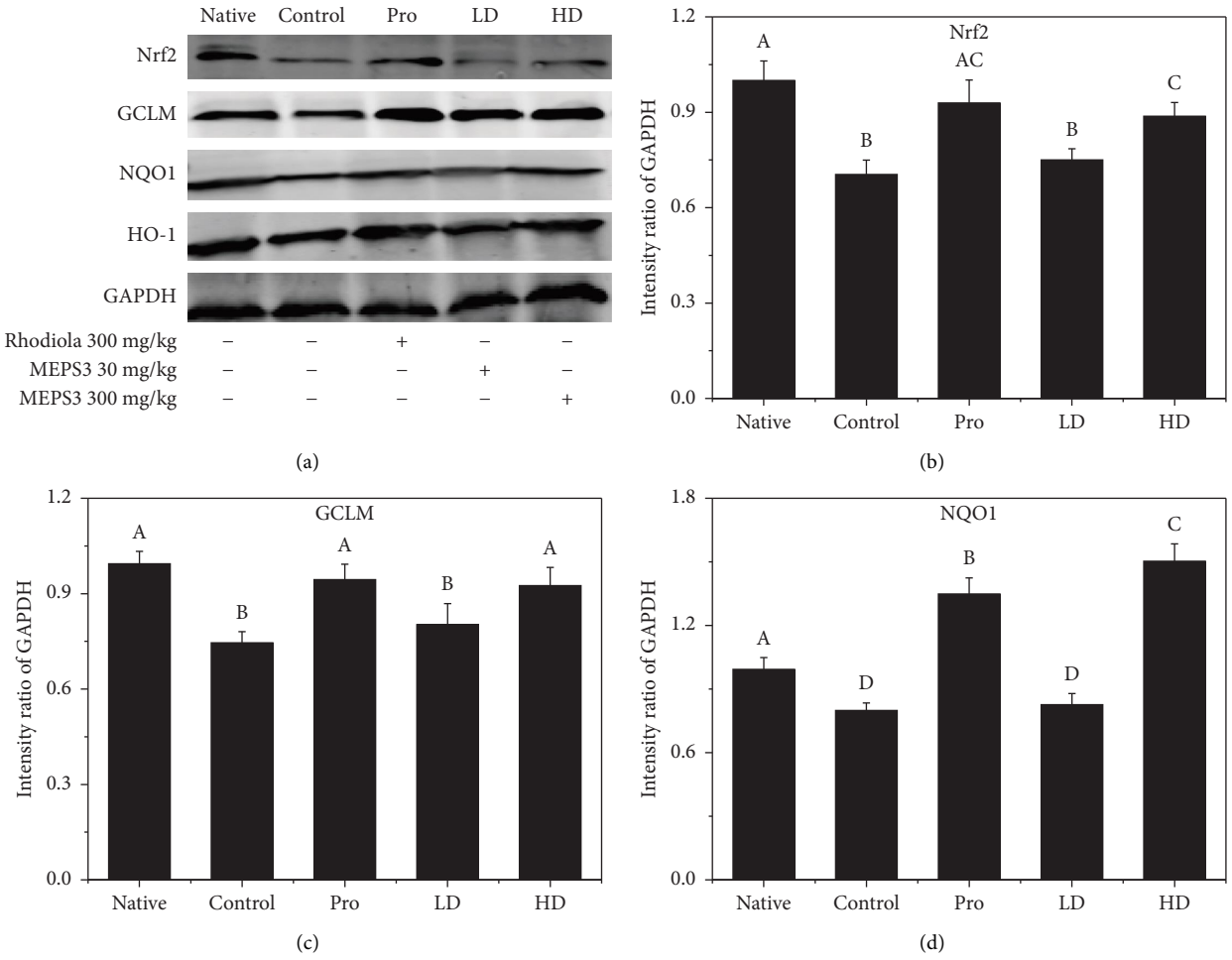

Figure 7: Continued.

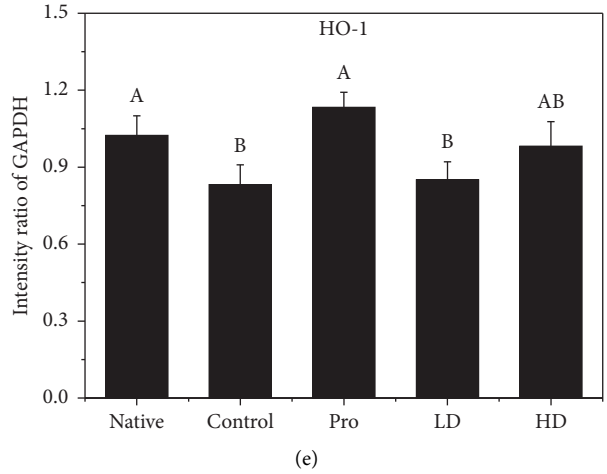

Figure 7: Effects of Rhodiola (300 mg/kg, i.g.) and MEPS3 (30 and 300 mg/kg, i.g.) on Nrf-2 signaling (a) and its downstream key proteins Nrf2 (b), GCLM (c), NQO1 (d), and HO-1 (e). Data are expressed as the mean ± S.D. (AD) Bars with different superscripts are significantly different ($P < 0.05$). Pro, administered Rhodiola); LD, administered a low dose of MEPS3; and HD, administered a high dose of MEPS3.

In this study, MEPS3 supplementation increased the levels of key proteins of the Nrf-2/ARE pathway, such as Nrf2, GCLM, NQO1, and HO-1, which indicated that MEPS3 exerts an antifatigue effect through the Nrf-2/ARE pathway.

4. Conclusion

In this study, MEPS3 treatment significantly increased the rotarod and swimming times by 38.9 and 49.2%, respectively, while reducing the electric shock time by 48.05% compared to those in the vehicle group. These results indicated that MEPS3 exhibited the highest antifatigue capacity. In addition, the results showed that the molecular weight of MEPS3 was 10.47 kDa. Monosaccharide analysis indicated that MEPS3 consists of mannose, glucose, and galactose in a molar ratio of 0.08 : 0.34 : 1.46. The uronic acid content in MEPS3 was 4.2%. Infrared spectra analysis showed the presence of uronic acid, pyranose ring, and β-chain glycosyl residues in MEPS3. NMR experiments confirmed the results of monosaccharide analysis. We found that MEPS3 exerts an antifatigue effect by reducing LA and ROS levels and increasing the plasma LDH activity. Oxidative stress is closely related to fatigue, and MEPS3 regulates oxidative stress via the Nrf-2 signaling pathway. These results provide valuable insights into the antifatigue mechanism, highlighting MEPS3 as a novel and readily accessible natural antifatigue agent. Our findings offer experimental evidence supporting the potential clinical use of MEPS3 as an effective agent against fatigue. MEPS3 holds promise as a functional food or drug for managing fatigue.

Data Availability

The data used to support the findings of this study are included within the article.

Ethical Approval

All animal procedures were performed in accordance with the Guidelines for Care and Use of Laboratory Animals (Ministry of Science and Technology of China, 2006) and were approved by the Institutional Animal Committee of Qilu University of Technology (QLU20200625).

Disclosure

Peng Du and Nan Li share the first authorship.

Conflicts of Interest

The authors declare that they have no conflicts of interest.

Authors' Contributions

Peng Du and Nan Li contributed equally to this work.

Acknowledgments

The products and services were provided by Beijing Boxbio Science and Technology Co., Ltd. This research was funded by the Key R & D Program of Shandong Province (2020CXGC010603).

Supplementary Materials

Table S1 summarizes the main proton and carbon signals. Figure S1 shows the FT-IR spectra of MEPS3. (*Supplementary Materials*)

References

[1] F. Meng, G. Xing, Y. Li et al., "The optimization of Marasmius androsaceus submerged fermentation conditions in five-liter fermentor," *Saudi Journal of Biological Sciences*, vol. 23, no. 1, pp. S99–S105, 2016.

[2] K. Huang, Y. Li, S. Tao et al., "Purification, characterization and biological activity of polysaccharides from dendrobium officinale," *Molecules*, vol. 21, no. 6, p. 701, 2016.

[3] L. Zhang, M. Yang, Y. Song et al., "Antihypertensive effect of 3,3,5,5-tetramethyl-4-piperidone, a new compound extracted from Marasmius androsaceus," *Journal of Ethnopharmacology*, vol. 123, no. 1, pp. 34–39, 2009.

[4] X. Li, H. Zhang, and H. Xu, "Analysis of chemical components of shiitake polysaccharides and its anti-fatigue effect under vibration," *International Journal of Biological Macromolecules*, vol. 45, no. 4, pp. 377–380, 2009.

[5] R. E. Keyser, "Peripheral fatigue: high-energy phosphates and hydrogen ions," *PM&R*, vol. 2, no. 5, pp. 347–358, 2010.

[6] Q. Xie, Y. Sun, L. Cao et al., "Antifatigue and antihypoxia activities of oligosaccharides and polysaccharides from Codonopsis pilosula in mice," *Food & Function*, vol. 11, no. 7, pp. 6352–6362, 2020.

[7] A. Chi, H. Li, C. Kang et al., "Anti-fatigue activity of a novel polysaccharide conjugates from Ziyang green tea," *International Journal of Biological Macromolecules*, vol. 80, no. 1, pp. 566–572, 2015.

[8] H. Gao, W. Zhang, B. Wang et al., "Purification, characterization and anti-fatigue activity of polysaccharide fractions from okra (Abelmoschus esculentus (L.) Moench)," *Food & Function*, vol. 9, no. 2, pp. 1088–1101, 2018.

[9] M. Zhu, H. Zhu, X. Ding, S. Liu, and Y. Zou, "Analysis of the anti-fatigue activity of polysaccharides from Spirulina platensis: role of central 5-hydroxytryptamine mechanisms," *Food & Function*, vol. 11, no. 2, pp. 1826–1834, 2020.

[10] W. D. Shen, X. Li, Y. Deng et al., "Polygonatum cyrtonema Hua polysaccharide exhibits anti-fatigue activity via regulating osteocalcin signaling," *International Journal of Biological Macromolecules*, vol. 175, no. 4, pp. 235–241, 2021.

[11] J. Song, X. Geng, Y. Su et al., "Structure feature and antidepressant-like activity of a novel exopolysaccharide isolated from Marasmius androsaceus fermentation broth," *International Journal of Biological Macromolecules*, vol. 165, no. 3, pp. 1646–1655, 2020.

[12] G. T. Chen, B. Yuan, H. X. Wang, G. H. Qi, and S. J. Cheng, "Characterization and antioxidant activity of polysaccharides obtained from ginger pomace using two different extraction processes," *International Journal of Biological Macromolecules*, vol. 139, no. 2, pp. 801–809, 2019.

[13] S. Palanisamy, M. Vinosha, T. Marudhupandi, P. Rajasekar, and N. M. Prabhu, "In vitro antioxidant and antibacterial activity of sulfated polysaccharides isolated from Spatoglossum asperum," *Carbohydrate Polymers*, vol. 170, no. 4, pp. 296–304, 2017.

[14] Y. Liu, Y. You, Y. Li et al., "The characterization, selenylation and antidiabetic activity of mycelial polysaccharides from Catathelasma ventricosum," *Carbohydrate Polymers*, vol. 174, no. 3, pp. 72–81, 2017.

[15] W. S. Yi, L. H. Qin, and J. B. Cao, "Investigation of morphological change of green tea polysaccharides by SEM and AFM," *Scanning*, vol. 33, no. 6, pp. 450–454, 2011.

[16] J. Pi, Y. Wang, H. Zhu et al., "Immunomodulatory effects of polysaccharide compounds in macrophages revealed by high resolution AFM," *Scanning*, vol. 38, no. 6, pp. 792–801, 2016.

[17] P. Du, J. Song, H. Qiu et al., "Polyphenols extracted from shanxi-aged vinegar inhibit inflammation in LPS-induced RAW264.7 macrophages and ICR mice via the suppression of MAPK/NF-κB pathway activation," *Molecules*, vol. 26, no. 9, p. 2745, 2021.

[18] J. H. Roh, I. G. Ko, S. E. Kim et al., "Treadmill exercise ameliorates intracerebral hemorrhage-induced depression in rats," *Journal of Exercise Rehabilitation*, vol. 12, no. 4, pp. 299–307, 2016.

[19] J. Wang, S. Li, Y. Fan et al., "Anti-fatigue activity of the water-soluble polysaccharides isolated from Panax ginseng C. A. Meyer," *Journal of Ethnopharmacology*, vol. 130, no. 2, pp. 421–423, 2010.

[20] J. Liu, C. Du, Y. Wang, and Z. Yu, "Anti-fatigue activities of polysaccharides extracted from Hericium erinaceus," *Experimental and Therapeutic Medicine*, vol. 9, no. 2, pp. 483–487, 2015.

[21] J. Song, G. Xing, J. Cao et al., "Investigation of the antidepressant effects of exopolysaccharides obtained from Marasmius androsaceus fermentation in a mouse model," *Molecular Medicine Reports*, vol. 13, no. 1, pp. 939–946, 2016.

[22] L. Bai, C. Tan, J. Ren et al., "Cordyceps militaris acidic polysaccharides improve learning and memory impairment in mice with exercise fatigue through the PI3K/NRF2/HO-1 signalling pathway," *International Journal of Biological Macromolecules*, vol. 227, pp. 158–172, 2023.

[23] W. H. Hsu, W. L. Qiu, S. M. Tsao et al., "Effects of WSG, a polysaccharide from Ganoderma lucidum, on suppressing cell growth and mobility of lung cancer," *International Journal of Biological Macromolecules*, vol. 165, pp. 1604–1613, 2020.

[24] M. Cai, H. Xing, B. Tian et al., "Characteristics and antifatigue activity of graded polysaccharides from Ganoderma lucidum separated by cascade membrane technology," *Carbohydrate Polymers*, vol. 269, Article ID 118329, 2021.

[25] J. H. Lim, K. M. Kim, S. W. Kim, O. Hwang, and H. J. Choi, "Bromocriptine activates NQO1 via Nrf2-PI3K/Akt signaling: novel cytoprotective mechanism against oxidative damage," *Pharmacological Research*, vol. 57, no. 5, pp. 325–331, 2008.

[26] J. Huo, J. Wu, W. Sun et al., "Immunomodulatory activity of a novel polysaccharide extracted from Huangshui on THP-1 cells through NO production and increased IL-6 and TNF-alpha expression," *Food Chemistry*, vol. 330, no. 1, Article ID 127257, 2020.

[27] J. Guan, F. Q. Yang, and S. P. Li, "Evaluation of carbohydrates in natural and cultured Cordyceps by pressurized liquid extraction and gas chromatography coupled with mass spectrometry," *Molecules*, vol. 15, no. 6, pp. 4227–4241, 2010.

[28] W. Tang, L. Jin, L. Xie et al., "Structural characterization and antifatigue effect in vivo of maca (lepidium meyenii walp) polysaccharide," *Journal of Food Science*, vol. 82, no. 3, pp. 757–764, 2017.

[29] X. Ding, Y. Hou, and W. Hou, "Structure feature and antitumor activity of a novel polysaccharide isolated from Lactarius deliciosus Gray," *Carbohydrate Polymers*, vol. 89, no. 2, pp. 397–402, 2012.

[30] M. Meng, D. Cheng, L. Han, Y. Chen, and C. Wang, "Isolation, purification, structural analysis and immunostimulatory activity of water-soluble polysaccharides from Grifola Frondosa fruiting body," *Carbohydrate Polymers*, vol. 157, no. 2, pp. 1134–1143, 2017.

[31] W. Ni, T. Gao, H. Wang et al., "Anti-fatigue activity of polysaccharides from the fruits of four Tibetan plateau indigenous medicinal plants," *Journal of Ethnopharmacology*, vol. 150, no. 2, pp. 529–535, 2013.

[32] Z. Gao, D. Kong, W. Cai, J. Zhang, and L. Jia, "Characterization and anti-diabetic nephropathic ability of mycelium polysaccharides from Coprinus comatus," *Carbohydrate Polymers*, vol. 251, no. 2, Article ID 117081, 2021.

[33] M. Karmakar, H. Mondal, M. Mahapatra, P. Chattopadhyay, S. Chatterjee, and N. Singha, "Pectin-grafted terpolymer superadsorbent via N-H activated strategic protrusion of monomer for removals of Cd(II), Hg(II), and Pb(II)," *Carbohydrate Polymers*, vol. 206, no. 2, pp. 778–791, 2019.

[34] H. Zhang, P. Zou, H. Zhao, J. Qiu, J. Regenstein, and X. Yang, "Isolation, purification, structure and antioxidant activity of polysaccharide from pinecones of Pinus koraiensis," *Carbohydrate Polymers*, vol. 251, no. 2, Article ID 117078, 2021.

[35] F. Li, Y. Wei, L. Liang, L. Huang, G. Yu, and Q. Li, "A novel low-molecular-mass pumpkin polysaccharide: structural characterization, antioxidant activity, and hypoglycemic potential," *Carbohydrate Polymers*, vol. 251, no. 2, Article ID 117090, 2021.

[36] X. Hu, K. Wang, M. Yu et al., "Characterization and antioxidant activity of a low-molecular-weight xanthan gum," *Biomolecules*, vol. 9, no. 11, p. 730, 2019.

[37] Y. Y. Feng, H. Y. Ji, X. D. Dong, and A. J. Liu, "An alcohol-soluble polysaccharide from Atractylodes macrocephala Koidz induces apoptosis of Eca-109 cells," *Carbohydrate Polymers*, vol. 226, no. 2, Article ID 115136, 2019.

[38] S. He, X. Wang, Y. Zhang et al., "Isolation and prebiotic activity of water-soluble polysaccharides fractions from the bamboo shoots (Phyllostachys praecox)," *Carbohydrate Polymers*, vol. 151, no. 1, pp. 295–304, 2016.

[39] Y. Sun, H. Wang, G. Guo, Y. Pu, and B. Yan, "The isolation and antioxidant activity of polysaccharides from the marine microalgae Isochrysis galbana," *Carbohydrate Polymers*, vol. 113, no. 4, pp. 22–31, 2014.

[40] X. Liang, Y. Gao, Y. Pan et al., "Purification, chemical characterization and antioxidant activities of polysaccharides isolated from Mycena dendrobii," *Carbohydrate Polymers*, vol. 203, no. 3, pp. 45–51, 2019.

[41] F. Xu, R. C. Sun, M. Z. Zhai et al., "Fractional separation of hemicelluloses and lignin in high yield and purity from mild ball-milled Periploca sepium," *Separation Science and Technology*, vol. 43, no. 11-12, pp. 3351–3375, 2008.

[42] I. F. Olawuyi and W. Y. Lee, "Structural characterization, functional properties and antioxidant activities of polysaccharide extract obtained from okra leaves (Abelmoschus esculentus)," *Food Chemistry*, vol. 354, no. 2, Article ID 129437, 2021.

[43] H. Peng, N. Wang, Z. R. Hu et al., "Physicochemical characterization of hemicelluloses from bamboo (Phyllostachys pubescens Mazel) stem," *Industrial Crops and Products*, vol. 37, no. 1, pp. 41–50, 2012.

[44] L. C. Yang, T. J. Lu, C. C. Hsieh, and W. C. Lin, "Characterization and immunomodulatory activity of polysaccharides derived from Dendrobium tosaense," *Carbohydrate Polymers*, vol. 111, no. 2, pp. 856–863, 2014.

[45] B. Liu, Z. Z. Shang, Q. M. Li et al., "Structural features and anti-gastric cancer activity of polysaccharides from stem, root, leaf and flower of cultivated Dendrobium huoshanense," *International Journal of Biological Macromolecules*, vol. 143, no. 4, pp. 651–664, 2020.

[46] L. C. Yang, C. C. Hsieh, and W. C. Lin, "Characterization and immunomodulatory activity of rice hull polysaccharides," *Carbohydrate Polymers*, vol. 124, no. 4, pp. 150–156, 2015.

[47] I. S. Bushmarinov, O. G. Ovchinnikova, N. A. Kocharova et al., "Structure of the O-polysaccharide from the lipopolysaccharide of Providencia alcalifaciens O29," *Carbohydrate Research*, vol. 341, no. 9, pp. 1181–1185, 2006.

[48] C. Y. Hsiao, Y. J. Hsu, Y. T. Tung, M. C. Lee, C. C. Huang, and C. C. Hsieh, "Effects of Antrodia camphorata and Panax ginseng supplementation on anti-fatigue properties in mice," *Journal of Veterinary Medical Science*, vol. 80, no. 2, pp. 284–291, 2018.

[49] Q. Yang, W. Jin, X. Lv et al., "Effects of macamides on endurance capacity and anti-fatigue property in prolonged swimming mice," *Pharmaceutical Biology*, vol. 54, no. 5, pp. 827–834, 2016.

[50] L. Z. Huang, B. K. Huang, Q. Ye, and L. P. Qin, "Bioactivity-guided fractionation for anti-fatigue property of Acanthopanax senticosus," *Journal of Ethnopharmacology*, vol. 133, no. 1, pp. 213–219, 2011.

[51] P. Du, J. Zhou, L. Zhang et al., "GC × GC-MS analysis and hypolipidemic effects of polyphenol extracts from Shanxi-aged vinegar in rats under a high fat diet," *Food & Function*, vol. 11, no. 9, pp. 7468–7480, 2020.

[52] N. Wakabayashi, S. L. Slocum, J. J. Skoko, S. Shin, and T. W. Kensler, "When NRF2 talks, who's listening?" *Antioxidants and Redox Signaling*, vol. 13, no. 11, pp. 1649–1663, 2010.